

# Green wideband RFID tag antenna for supply chain applications

Yasar Amin<sup>1a)</sup>, Rajeev Kumar Kanth<sup>2</sup>, Pasi Liljeberg<sup>2</sup>,  
Qiang Chen<sup>1</sup>, Li-Rong Zheng<sup>1</sup>, and Hannu Tenhunen<sup>1,2</sup>

<sup>1</sup> iPack VINN Excellence Center, Royal Institute of Technology (KTH)  
Isafjordsgatan 39, Stockholm, SE-16440, Sweden

<sup>2</sup> TUCS, Department of Information Technology, University of Turku  
Turku-20520, Finland

a) [ysar@kth.se](mailto:ysar@kth.se)

**Abstract:** In this paper, we demonstrate for the first time an RFID tag antenna manufactured by advanced inkjet printing technology on paper substrate using novel hole-matching technique for reducing the consumption of substrate material and conductive ink while attaining green RFID tags. In-depth electromagnetic analysis is performed methodologically for optimizing the parameters that effectuate the antenna dimensions. The antenna design is optimized for consistent wideband performance and extended read range throughout the complete UHF RFID band (860–960 MHz), while exhibiting benchmarking results when n across cardboard cartons filled with metal or water containing objects.

**Keywords:** RFID tag, wideband antenna, inkjet printing, paper substrate, green electronics

**Classification:** Microwave and millimeter wave devices, circuits, and systems

## References

- [1] Y. Zuo, “Survivable RFID systems: issues, challenges, and techniques,” *IEEE Trans. Syst. Man, Cybern. C, Appl. Rev.*, vol. 40, no. 4, pp. 406–418, July 2010.
- [2] G. M. Gaukler, “Item-level RFID in a retail supply chain with stock-out-based substitution,” *IEEE Trans. Ind. Informat.*, vol. 7, no. 2, pp. 362–370, May 2011.
- [3] K. V. S. Rao, P. V. Nikitin, and S. F. Lam, “Antenna design for UHF RFID tags: a review and a practical application,” *IEEE Trans. Antennas Propag.*, vol. 53, no. 12, pp. 3870–3876, Dec. 2005.
- [4] I. Bose and S. Yan, “The green potential of RFID projects: a case-based analysis,” *IT Professional*, vol. 13, no. 1, pp. 41–47, Jan.-Feb. 2011.

## 1 Introduction

Passive radio frequency identification (RFID) has recently engrossed much attention from retailers and manufacturers in all areas of the supply chain [1, 2]. It is a contactless identification technique that transmits data from an identification tag to a reader device via electromagnetic waves by obeying backscattering principle [3]. Presently majority of the RFID circuits are fabricated on nonbiodegradable substances i.e., FR-4 or PET. In order for businesses to minimize their impact on the environment, there is a need to limit this adversely challenging factor [4].

This paper presents eco-friendly wideband (860–960 MHz) RFID tag antenna inkjet printed on commercially available paper substrate. We have addressed the newfangled set of parameters emerging in RFID antennas while entering the era of green RFID revolution by evaluating and optimizing the key design parameters which are affected by the utilization of paper substrate. The proposed antenna uses innovative technique of square pattern holes for conjugately impedance matching with the RFID chip, thus eliminating the use of matching network and reduces the ink usage. The proposed tag is a perfect choice for far-field industrial applications especially for large items-level tracking in supply chain (cardboard cartons containing water & metal objects) and freight (wood or metal pallet) transportation.

## 2 Antenna design analysis and optimization

The proposed antenna is optimized in an organized approach for maximizing the read range while minimizing the ink consumption. One of the critical observations made while field testing (in supply chain industry) of antennas having thinner traces used for matching network, is that the effect of even minor scratches on those tracks can cause loss of RFID tags during transportation. Therefore, it led us towards the realization of a structure which can eliminate such risk factors while exhibiting better performance. Design computations and optimizations are performed using ANSYS HFSS<sup>TM</sup> for the target IC NXP UCODE G2XM (13.3-j122 Ω@915 MHz). The substrate adopted is Kodak photopaper of 250 μm thickness (280 gm/m<sup>2</sup>) with dielectric permittivity of  $\epsilon_r = 3.2$ , and loss tangent  $\tan \delta = 0.077$ , characterized at 1 GHz@25°C. The primary aim of parametric optimization is to maximize the feeding power to the load (IC). An often neglected issue during designing an (RFID) antenna is how directivity and gain are related to its physical dimensions. In view of the fact that the field/current, on the antenna aperture is not uniform, the parametric optimization of antenna effective aperture is carried out, as the effective aperture  $A_e$  is less than the physical aperture  $A_p$ . The directivity in terms of the aperture size and aperture efficiency is:

$$D = \frac{4\pi}{\lambda^2} A_e = \frac{4\pi}{\lambda^2} \eta_{ap} A_p \quad (1)$$

It is observed that  $\eta_{ap}$  is generally 50 to 80%. By knowing the power density  $S$  at the receiving antenna, we have estimated the received power at the tag:

$$P_r = S A_e \quad (2)$$

Hence during optimization strategy, much effort is devoted for improving the effective aperture in order to boost the antenna gain which consequently increases the amount of power delivered to the chip.

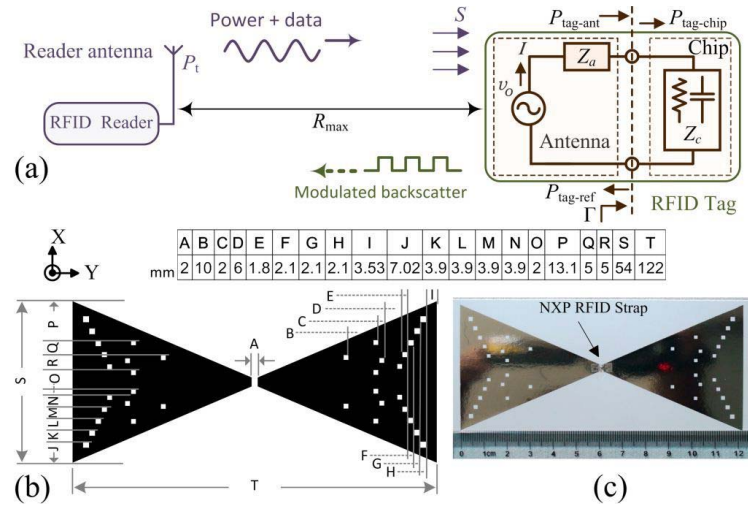


**Fig. 1.** (a) Far-field RFID mechanism & tag equivalent circuit; (b) geometry & dimensions of proposed antenna; (c) printed tag on paper.

Now by achieving maximum effective aperture  $A_{e-max}$  of the tag antenna located in the field of the reader antenna with the power density  $S$  as showed in Fig. 1(a). The tag antenna receives the power from the wave and delivers it to the RFID chip (strap) with load impedance  $Z_c$ . Fraction of the power received by the tag antenna is delivered to the chip whereas the remaining portion of power is reflected and re-radiated by the antenna. Thus, the power transmission coefficient,  $\tau$  is used to calculate the power delivered to the RFID chip. Mathematically, it is expressed as:

$$P_{tag-chip} = \tau P_{tag-ant} \quad (3)$$

where  $P_{tag-ant}$  is the power antenna received from the incident wave, and  $P_{tag-chip}$  is the power delivered to the chip. The power transmission coefficient,  $\tau$ , is determined by the impedance matching between the tag antenna and the chip. Therefore, good impedance matching between antenna and chip is of paramount importance. In the Thevenin equivalent circuit of the tag showed in Fig. 1(a),  $Z_c = R_c + jX_c$  is the complex chip impedance and  $Z_a = R_a + jX_a$  is the complex antenna impedance. The  $Z_c$  takes in the effects of strap and chip package parasitics. It is worth mentioning here that both  $Z_a$  and  $Z_c$  are frequency-dependent. Power wave reflection coefficient  $\Gamma$  is defined to evaluate the transmission of the power waves as:

$$\Gamma = \frac{Z_c - Z_a^*}{Z_c + Z_a}, \quad 0 \leq |\Gamma| \leq 1 \quad (4)$$

Thus, the power delivered to the chip is:

$$P_{tag-chip} = (1 - |\Gamma|^2) P_{tag-ant} \quad (5)$$

Therefore, the power transmission coefficient is calculated by:

$$\tau = \frac{P_{tag-chip}}{P_{tag-ant}} = 1 - |\Gamma|^2 = \frac{4R_a R_c}{(R_a + R_c)^2 + (X_a + X_c)^2}, \quad 0 \leq \tau \leq 1 \quad (6)$$

From Eq. (5) maximum power is transferred when the antenna is conjugately matched to the chip, i.e.  $R_c = R_a$  and  $X_c = -X_a$ , then  $|\Gamma| = 0$ ,  $\tau = 1.0$ . After rigorously going through iterations based on this numerical analysis, we have achieved 20% compact structure than its counterpart T-matched design, and Eq. (2) takes the form:

$$P_{tag-chip-max} = P_{tag-ant} = S A_{e-max} \quad (7)$$

The skin depth is evaluated through:

$$\delta = \sqrt{\frac{1}{\pi f \mu \sigma}} \quad (8)$$

Thus, at UHF in accordance with Eq. (8), the conductive traces are made to obtain a thickness of the same order of magnitude as the skin depth. However, it is observed that in case the thickness is equal to or thinner than the skin depth, the total resistance of a printed conductive trace with fixed trace width is proportional to the overall trace length and inversely proportional to the conductor thickness.

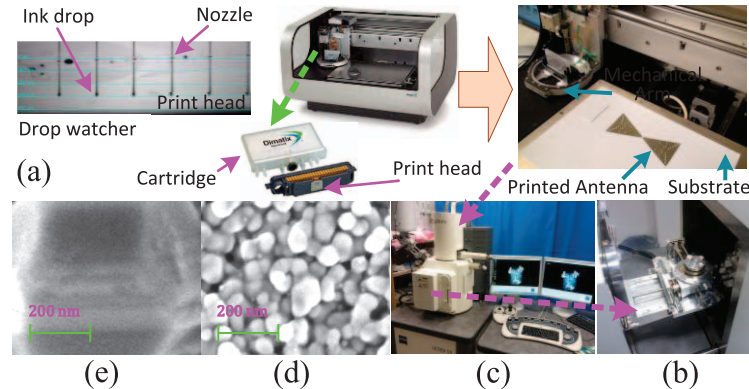


**Fig. 2.** (a) Inkjet printing setup; (b) SEM sample holder; (c) SEM setup; SEM images of three layers of printed silver nanoparticle ink, after curing 2hr at: (d) 100°C, (e) 150°C.

In previously reported results cavities were used in the antenna arms for either brand identification or ink saving, but in both cases this practice terminates into inferior current distribution in the antenna arms. However in the proposed antenna, the induction of pattern holes is effective for matching of the antenna impedance to that of the IC through the fine tuning of their location and size which is mentioned in Fig. 1(b) without deteriorating the current distribution. It is observed that earlier efforts to reduce the ink usage also led towards lower gain and as a result, the scope of those tags is limited

in supply chain industry. In the proposed procedure for achieving multidimensional performance benefits, the pattern holes suite these requirements effectively. It is noticed that the inner holes positions (B-D) are more persuasive towards antenna efficiency whereas, the outer hole positions (E-I) assist more towards fine tuning the impedance. The vertical holes positions (J-P) are critical towards current distribution. Therefore, this efficient technique in combination with above mentioned optimizing method not only fulfilled the matching criteria, but also reduced the conductive ink consumption by 35% without performance degradation.

The proposed structure is inkjet printed on paper substrate with print resolution of 1270 dpi by using silver nano-particle based ink (CCI-300 from Cabot Corp.) with Fujifilm Dimatix DMP 2800 printer as showed in Fig. 2(a). The resultant thickness of single layer of the printed trace is around 600 nm, which goaded to print three layers of the proposed antenna pattern (showed in Fig. 1(c)) in reference to limit the skin depth effect. After annealing, the characterization of the printed antenna structures is carried out under ULTRA-55 FESEM from Carl Zeiss NTS showed in Figures 2(b) & (c). Figures 2(d) & (e) show the SEMs for elaborating the difference between the heating temperatures. It is pragmatic under suitable annealing conditions 150°C/120 min, an almost solid metal conductor with measured conductivity of  $9 \times 10^6$ – $1.1 \times 10^7$  [S/m] is formed.

### 3 Field and circuit concepts parametric analysis

The characterization of reliability and repeatability is conducted by employing worst case analysis. Thus, for this reason maximum deviated values at a certain frequency are reported in impedance graphs. Impedance measurements are carried out with handheld (VNA) vector network analyzer (MS2026B, Anritsu) by using S-parameter measurement method. Figures 3(a) & (b) show the impedance plots. It is observed from Fig. 3(a) the computed and measured resistance for the antenna from 860–960 MHz varies between two extremes, from 13–15  $\Omega$  with mostly measured values maintain around 14  $\Omega$ . The reactance part of the impedance, as showed in Fig. 3(b), exhibits a positive value with a linear variation against frequency. The return loss of the proposed antenna is calculated based on the power reflection coefficient by using Eq. (4). Fig. 3(c) shows the measured and computed return loss of the proposed antenna with the measured bandwidth of the antenna in the worst case is 260 MHz, corresponding to 28% around the center frequency 910 MHz; so it covers the global UHF RFID bands and can cater greater degree of environmental disparities.

The read range measured by using Impinj's UHF RFID reader Kit validated that proposed tags exhibit consistent reading distance 7.5 meters and 9.3 meters while attached to cardboard cartons exclusively containing cola cans, and plastic water bottles, respectively. The radiation patterns are measured inside an anechoic chamber setup that replicates absolute free space. The antenna gain measurements are carried out by employing rigorous

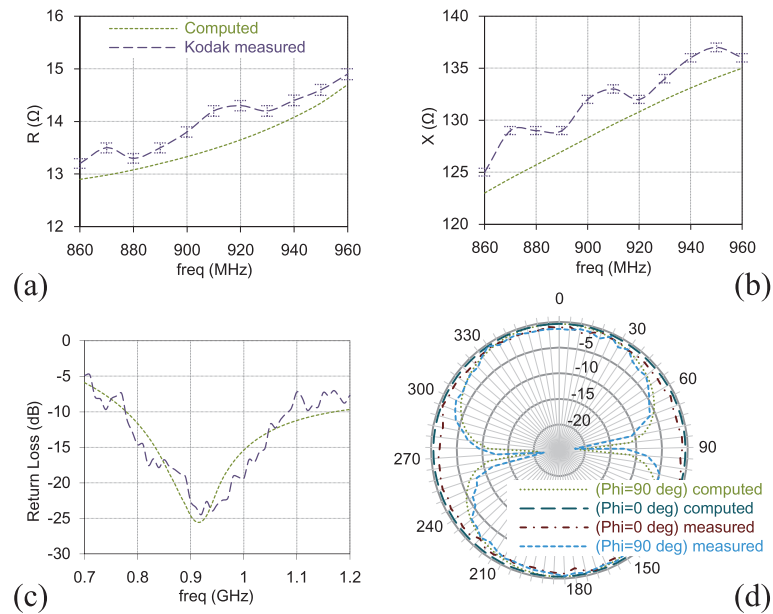


**Fig. 3.** (a) Resistance variation; (b) reactance variation; (c) measured & computed return loss; (d) 2D measured & computed far-field radiation plots.

three antennas measurement method, which proves surpassing directivity of 2.2 dBi despite the reduction in size and ink consumption. Fig. 3(d) shows the 2D measured normalized radiation patterns of antenna at characteristic frequency of 866 MHz. It is observed that radiation patterns are nearly uniform (omnidirectional) and show substantial concurrence between computations and measurements, which can also be established for other frequencies within the antenna bandwidth.

#### 4 Conclusion

To the best of our knowledge, this is the first time novel hole-matching technique is realized in combination with antenna effective aperture optimization method for enhancing the RFID tag performance on paper substrate. The intended meticulous optimization approach resulted into extended read range of up to 9.3 meters, 20% compact antenna size while cutting down the ink consumption by 35%. Thus, this approach will be a milestone for future development of green RFID tags. The proposed antenna is a perfect choice for roll-to-roll printing of ultra-low cost flexible tags for supply chain applications.

#### Acknowledgments

This work was financially supported by Vinnova (The Swedish Governmental Agency for Innovation Systems) through the Vinn Excellence centers program.